# Effect of site occupancy disorder on martensitic properties of $Mn_2NiIn$ type alloys: X-ray absorption fine structure study

D. N. Lobo, K. R. Priolkar, A. Koide, and S. Emura

Citation: Journal of Applied Physics **121**, 053902 (2017); doi: 10.1063/1.4975403
View online: http://dx.doi.org/10.1063/1.4975403
View Table of Contents: http://aip.scitation.org/toc/jap/121/5
Published by the American Institute of Physics

# Effect of site occupancy disorder on martensitic properties of $Mn_2NiIn$ type alloys: X-ray absorption fine structure study

D. N. Lobo,[1] K. R. Priolkar,[1,a)] A. Koide,[2] and S. Emura[3]
[1]*Department of Physics, Goa University, Taleigao Plateau, Goa 403 206, India*
[2]*Department of Materials Molecular Science, Institute of Molecular Science, Myodaiji-cho, Okazaki, Aichi 444-8585, Japan*
[3]*Institute of Scientific and Industrial Research, Osaka University, 8-1 Mihogaoka, Ibaraki, Osaka 567-0047, Japan*

(Received 30 November 2016; accepted 10 January 2017; published online 3 February 2017)

We have carried out *ab-initio* calculations of the local structure of Mn and Ni in the $Mn_2Ni_{1.5}In_{0.5}$ alloy with different site occupancies in order to understand the similarities in martensitic and magnetic properties of $Mn_2Ni_{1+x}In_{1-x}$ and $Ni_2Mn_{1+x}In_{1-x}$ alloys. Our results show that in $Mn_2Ni_{1+x}In_{1-x}$ alloys, there is a strong possibility of Mn atoms occupying all the three X, Y, and Z sites of the $X_2YZ$ Heusler structure, while Ni atoms preferentially occupy the X sites. Such a site occupancy disorder of Mn atoms is in addition to a local structural disorder due to size differences between Mn and In atoms, which is also present in $Ni_2Mn_{1+x}In_{1-x}$ alloys. Further, a comparison of the calculations with experimental x-ray absorption fine structure at the Mn and Ni K edges in $Mn_{2-y}Ni_{1.6+y}In_{0.4}$ ($-0.08 \le y \le 0.08$) indicates a strong connection between martensitic transformation and occupancy of Z sites by Mn atoms. *Published by AIP Publishing.*
[http://dx.doi.org/10.1063/1.4975403]

## I. INTRODUCTION

Mn rich Ni-Mn-Z (Z = Ga, In, Sn, or Sb) type shape memory alloys have been studied for their novel properties such as giant reverse magneto-caloric effect,[1–17] large magnetic field induced strain,[18–23] magnetic superelasticity,[24] and complex magnetic order.[25–31] The origin of all these effects lies in a strong coupling between structural and magnetic degrees of freedom. Therefore, understanding the magnetic interactions between the constituent atoms as the alloys transform structurally gains importance. Despite several attempts, the understanding of the magnetism of the martensitic state is still elusive. Though the magnetic moment in Ni-Mn based Heusler alloys is almost entirely due to Mn atoms,[32–34] factors like antisite disorder,[35] changes in bond distances due to structural transformation,[36] and local structural disorder[37] bring in newer magnetic interactions and add to the complexities of the problem.

Increasing the Mn content in $Ni_{2-x}Mn_{1+x}Z$ (Z = Ga, In, Sn, Sb) alloys and at the same time preserving the Heusler structure result in alloys of type $Mn_2NiZ$. Band structure calculations have indicated such alloys to be ferrimagnetic due to unequal magnetic moments of antiferromagnetically coupled Mn atoms occupying the X and Y sites of the $X_2YZ$ Heusler structure.[38–42] Though martensitic transformation has been observed in $Mn_2NiGa$ ($T_M \sim 270$ K and $T_C = 588$ K),[39] the same is not observed in other $Mn_2NiZ$ alloys where Z = In or Sn. However, the increasing Ni content at the expense of Z atoms to realize alloys of the type $Mn_2Ni_{1+x}Z_{1-x}$ leads to martensitic instability in them.[43–45]

In the $L2_1$ Heusler composition, Ni atoms are believed to prefer X sites.[46] According to this premise in $Mn_2Ni_{1+x}Z_{1-x}$ alloys, if Ni atoms preferentially occupy X sites, a proportionate amount of Mn atoms would be forced to occupy Z sites, leading to what is known as site occupancy disorder. Such a disorder is known to introduce competing ferromagnetic and antiferromagnetic interactions between Mn atoms occupying the Y sublattice (Mn(Y)) and Mn atoms occupying the Z sublattice (Mn(Z)), leading to observation of exotic properties such as exchange bias effect in the zero field cooled (ZFC) state and spin valve effect in these Mn rich martensitic alloys.[47–49]

In our recent work,[45] the magnetic properties of $Mn_2Ni_{1+x}Z_{1-x}$ alloys in the martensitic state were found to be similar to those of $Ni_2Mn_{1+x}In_{1-x}$, and this was conjectured to be due to site occupancy disorder arising out of the preferential occupation of X sites by Ni atoms. But this general picture could not explain the complete suppression of martensitic transformation in $Mn_{2-y}Ni_{1.6+y}In_{0.4}$ due to a small increase in the Mn concentration at the expense of Ni ($-0.1 < y < 0$).[45] This is especially important because the alloy with $y = 0$ is martensitic with a transformation temperature of $\sim$230 K, which increases with an increase in the Ni concentration ($y > 0$). Hence, it becomes necessary to understand the correlation between the perceived site occupancy disorder in $Mn_2Ni_{1+x}In_{1-x}$ alloys and the observed similarity in martensitic and magnetic properties of these alloys with those of $Ni_2Mn_{1+x}In_{1-x}$ alloys at a microscopic level. To achieve this objective, here we report *ab-initio* calculations of Ni and Mn K edge x-ray absorption fine structure (XAFS) in prototypical $Mn_2Ni_{1.5}In_{0.5}$ using the FEFF 8.4 program and its comparison with experimental results obtained in $Mn_2Ni_{1.5}In_{0.5}$ and $Mn_{2-y}Ni_{1.6+y}In_{0.4}$ ($-0.08 \le y \le 0.08$).

a)Author to whom correspondence should be addressed. Electronic mail: krp@unigoa.ac.in

## II. METHODS

The samples of the above composition were prepared by arc melting the weighed constituents in an argon atmosphere followed by encapsulating in an evacuated quartz tube and annealing at 750 °C for 48 h and subsequent quenching in ice cold water. The prepared alloys were cut in suitable sizes using a low speed diamond saw, and part of the sample was powdered and re-annealed using the same procedure above. X-ray diffraction (XRD) patterns were recorded at room temperature in the angular range of $20^\circ \leq 2\theta \leq 100^\circ$ and were found to be single phase.[45] Magnetization measurements were performed in the temperature interval of 5 K–400 K using a vibrating sample magnetometer in the 100 Oe applied field during the zero field cooled (ZFC) and subsequent field cooled cooling (FCC) and field cooled warming (FCW) cycles.

XAFS at Ni K and Mn K edges was recorded at Photon Factory using beamline 12C at room temperature. For XAFS measurements, the samples to be used as absorbers, were ground to a fine powder, and uniformly distributed on a scotch tape. These sample coated strips were adjusted in number such that the absorption edge jump gave $\Delta\mu t \leq 1$, where $\Delta\mu$ is the change in the absorption coefficient at the absorption edge and $t$ is the thickness of the absorber. The incident and transmitted photon energies were simultaneously recorded using gas-ionization chambers as detectors. Measurements were carried out from 300 eV below the edge energy to 1000 eV above it with a 5 eV step in the pre-edge region and 2.5 eV step in the XAFS region. At each edge, at least three scans were collected to average statistical noise.

FEFF 8.4 software based on the self-consistent real-space multiple-scattering formalism[50] was employed for calculation of XAFS oscillations at the Mn K and Ni K edges in a prototypical alloy, $Mn_2Ni_{1.5}In_{0.5}$. Not only this alloy composition is close to the experimentally studied compositions but also the constituent atoms have a nonfractional number of near neighbors. For the FEFF calculations, spherical muffin tin potentials were self consistently calculated over a radius of 5 Å. Default overlapping muffin tin potentials and Hedin-Lunqvist exchange correlations were used to calculate x-ray absorption transitions to a fully relaxed final state in the presence of a core hole. Calculations were carried out for Mn K and Ni K edges assuming the $L2_1$ type Heusler structure. Two possible structural models and their variations that are explained in detail Section III were considered. XAFS was calculated for absorbing atoms at occupying X, Y, and Z sites of the Heusler structure and combined together by multiplying each site XAFS with an appropriate weighting fraction. During calculations, the amplitude reduction factor, $S_0^2$, was fixed to 0.8 and the $\sigma^2$ for respective paths was calculated considering a Debye temperature of 320 K (Ref. 51) and the spectrum temperature of 300 K.

## III. RESULTS AND DISCUSSION

Figure 1 presents the magnetization measurements carried out in the temperature range $5\,K \leq T \leq 400\,K$ in $Mn_{2-y}Ni_{1.6+y}In_{0.4}$ (y = 0.08, 0, and −0.08). It can be clearly seen that the alloys with y = 0 and 0.08 undergo martensitic transformation at about 230 K and 270 K, respectively. $Mn_{2.08}Ni_{1.52}In_{0.4}$ does not show any martensitic instability down to 5 K, thus highlighting a drastic change in martensitic transformation temperature with small changes in the alloy composition. A detailed study of magnetic properties of these alloys along with $Mn_2Ni_{1+x}In_{1-x}$ (x = 0.5, 0.6, and 0.7) has been already presented in Ref. 45. To understand these changes in martensitic transformation temperature, experimental XAFS data recorded at the Mn K and Ni K edges at room temperature in each of these alloys have been compared with calculated Mn and Ni XAFS data using FEFF.

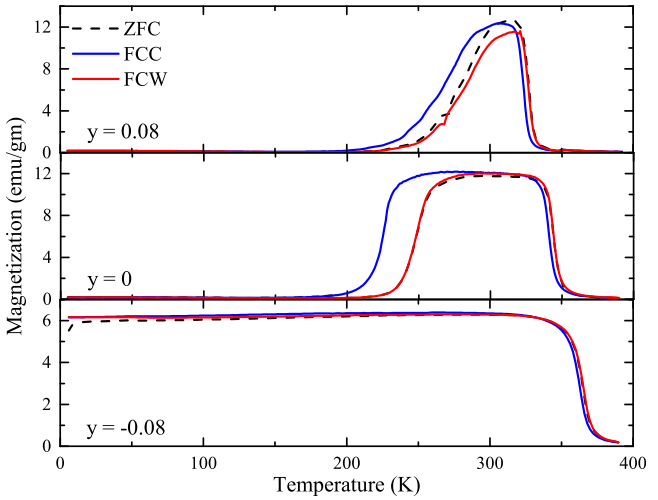


FIG. 1. Magnetization as a function of temperature for $Mn_{2-y}Ni_{1.6+y}In_{0.4}$ (y = 0.08, 0, and −0.08) measured in an applied field of 100 Oe during ZFC, FCC, and FCW cycles.

For the *ab-initio* calculations of Mn K and Ni K edge XAFS in the $Mn_2Ni_{1.5}In_{0.5}$ alloy, two structural models, designated as MODEL A and MODEL B, were considered. In MODEL A, the X sites of $X_2YZ$ are occupied equally by Ni and Mn, while all the Y sites are occupied by Mn and In and the remaining Ni atoms occupy the Z sites. In MODEL B, the entire fraction of Ni atoms occupies the X sites, forcing the proportionate amount of Mn atoms to occupy the Z sites along with Y sites, thus resulting in Mn occupying all the three X, Y, and Z sites in different fractions. The site occupancies in both these models are tabulated in Table I.

In Figure 2, calculated spectra at the Ni and Mn K edges according to MODEL A and MODEL B are compared with the experimental data recorded at room temperature. It is

TABLE I. Assumed site occupancies of X, Y, and Z sites of the $X_2YZ$ Heusler structure in MODEL A and MODEL B used for XAFS calculations of $Mn_2Ni_{1.5}In_{0.5}$.

| Sites | MODEL A | MODEL B | MODEL B1 | MODEL B2 |
|---|---|---|---|---|
| X | Ni | $Ni_{1.5}$ | $Ni_{1.5}$ | Ni |
| | Mn | $Mn_{0.5}$ | $Mn_{0.5}$ | Mn |
| Y | Mn | Mn | $Mn_{0.75}$ | $Mn_{0.5}$ |
| | | | $In_{0.25}$ | $Ni_{0.5}$ |
| Z | $Ni_{0.5}$ | $Mn_{0.5}$ | $Mn_{0.75}$ | $Mn_{0.5}$ |
| | $In_{0.5}$ | $In_{0.5}$ | $In_{0.25}$ | $In_{0.5}$ |

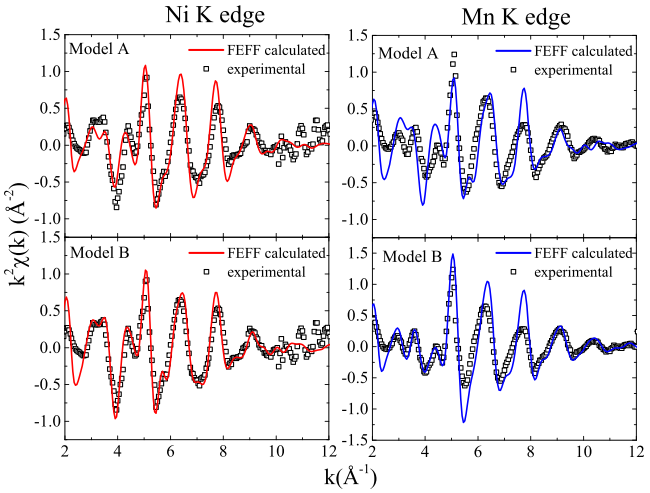


FIG. 2. Calculated Ni and Mn K edge XAFS for MODEL A and MODEL B along with experimental data.

observed that the oscillatory parts of the experimental Mn and Ni K edge XAFS spectra are reproduced by the two theoretical models. The calculated Ni K XAFS spectra of MODEL B give a much better description with the experimental data for the entire $k$ range under consideration than MODEL A. A similar conclusion could also be drawn for the calculated Mn K spectra although one can observe a mismatch between experimental and calculated Mn K XAFS spectra especially in the region between 5 and 8 $Å^{-1}$. In general, the better agreement of calculated spectra from MODEL B with the experimental XAFS spectra agrees well with the literature reports that support the case of Ni atoms preferentially occupying X sites.[39,48,52] These reports also indicate a disorder in occupancy of Mn atoms at different sites. Such a site occupancy disorder could be the reason for observed mismatch between the experimental and calculated spectra as per MODEL B. The site disorder in occupancy of Mn atoms was introduced in MODEL B in two different ways: MODEL B1 and MODEL B2. Their site occupancies of the X, Y, and Z sites are detailed in Table I.

Another reason for observed mismatch between experimental and calculated XAFS spectra could be incorrect estimation of $\sigma^2$. This is because the Debye temperature of $Mn_2NiIn$ alloys has not been reported in the literature and the value of 320 K chosen for the present calculations is the one reported for Ni-Mn-Ga alloys. It must be mentioned here that the measured values of Debye temperature for isostructural Heusler alloys containing Mn are reported to lie between 220 K and 320 K (Ref. 53), and hence, the present choice of Debye temperature may not be far from the true value. Also, the other extreme choice of 220 K does not significantly affect the calculated spectra.

The calculated Mn K edge EXAFS of MODELS B, B1, and B2 along with the experimental data has been plotted in Figs. 3(a), 3(b), and 3(c), respectively. A comparison of the calculated Mn K edge XAFS spectra with the experimental data does not conclusively suggest any one of these models to be a better descriptor of experimental data.

In $Ni_2Mn_{1+x}In_{1-x}$ alloys, a local structural distortion especially in the position of Mn atoms at the Z site (Mn(Z)) was shown to be responsible for the martensitic transformation for $x > 0.3$.[54] Since in MODEL B, both Mn and In atoms occupy the Z sites, a similar local structural distortion can exist in $Mn_2Ni_{1+x}In_{1-x}$ alloys, resulting in a shorter Mn(Z)-X bond as compared to the In-X bond. Such a distortion was introduced by tweaking the coordinates of Mn(Z) atoms in the FEFF input file. The coordinates of Mn(Z) atoms in

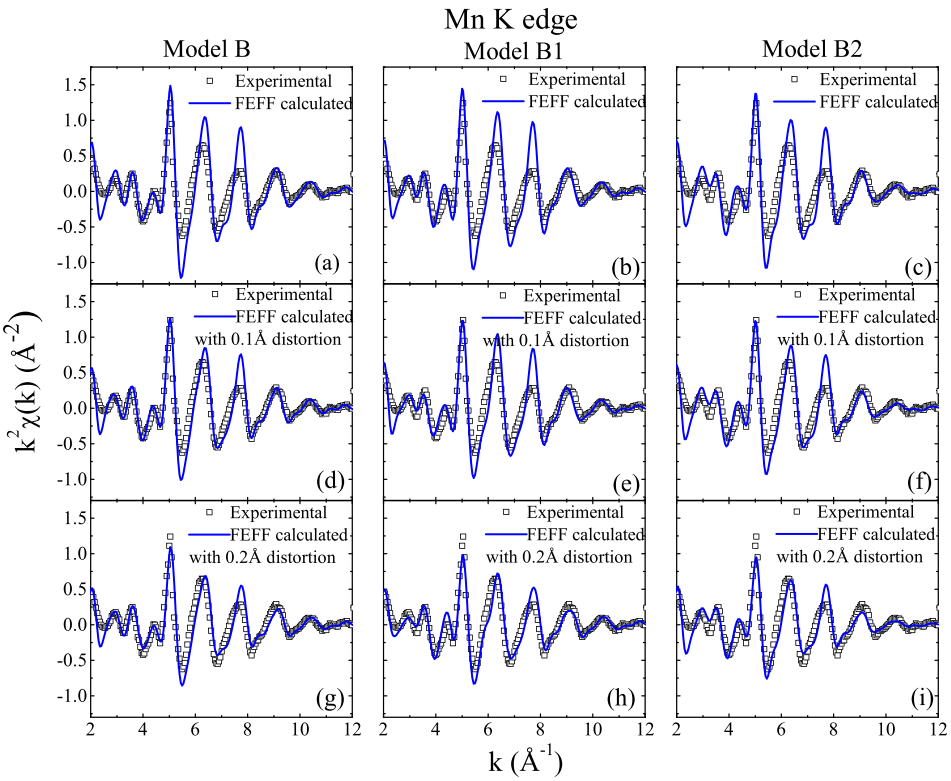


FIG. 3. Comparison of experimental XAFS data at the Mn K edge with the calculated Mn K edge XAFS for MODELS B, B1, and B2 for an undistorted lattice ((a)–(c)) and for a lattice with local structural distortion, wherein Mn atoms at the Z site are displaced closer to X sites by 0.1 Å ((d)–(f)) and 0.2 Å ((g)–(i)).

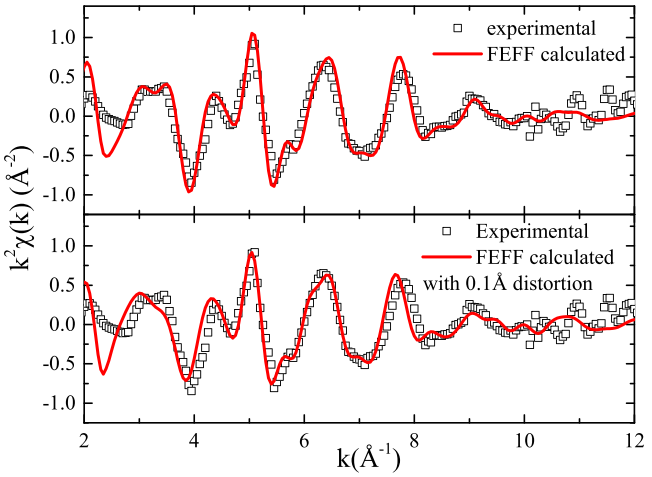


FIG. 4. Ni K edge XAFS data calculated as for MODEL B for (a) an undistorted lattice and (b) a lattice with local structural distortion, wherein Mn atoms at the In site are displaced closer to X site atoms by 0.1 Å.

MODELS B, B1, and B2 were changed in such a way that they were closer to X site atoms by 0.1 Å and 0.2 Å as compared to the In atoms occupying the Z sites. Figs. 3(d)–3(f) and 3(g)–3(i) show the comparison for MODELS B, B1, and B2 at the Mn K edge EXAFS with experimental data for local structure distortion of 0.1 Å and 0.2 Å, respectively, in the k range from 2 to 12 $Å^{-1}$.

From Fig. 3, it is observed that with increasing disorder from 0.1 Å to 0.2 Å for all three models, the amplitude of calculated EXAFS oscillations for all models reduces and tends towards the experimental data, which is an indication of the presence of local structure disorder in these alloys. Since all the alloys have long range structural order as evidenced from Bragg reflections in x-ray diffraction data, a displacement of a particular atom by 0.2 Å from its crystallographic site position may be a bit unrealistic. Hence, models with 0.1 Å displacement of Mn(Z) atoms were taken to provide the most realistic description of site occupancies in such $Mn_2Ni_{1+x}In_{1-x}$ alloys. Of the three, MODEL B was preferred over MODELS B1 and B2 due to its relative simplicity. Irrespective of the choice of models, the present analysis clearly suggests antisite disorder along with local structural disorder to be primarily responsible for physical properties of $Mn_2NiIn$ type alloys. Antisite disorder has also been reported to be responsible for exotic properties like spin valve effect and zero field exchange bias in related $Mn_2NiGa$ and $Mn_2PtGa$.[47,48]

The calculated Ni K edge XAFS plot for MODEL B with a local structure distortion of 0.1 Å also presents a better agreement with the experimental data as compared to the undistorted MODEL B (see Fig. 4). This confirms the presence of antisite disorder along with a local structural disorder in these $Mn_2NiIn$ type alloys. The presence of Mn at the Z sites could be the reason for similarity of magnetic properties in the martensitic state of $Mn_2Ni_{1+x}In_{1-x}$ and the magnetic properties of $Ni_2Mn_{1+x}In_{1-x}$ alloys in their martensitic state. In other words, an increase in the Ni content at the expense of In in Mn-Ni-In alloys causes Mn to occupy the Z sites due to preference of Ni atoms for X sites. Such a site occupancy coupled with local structural disorder favors the formation of Ni-Mn(Z) hybridization, which is responsible for martensitic transformation and antiferromagnetism in the martensitic state.

Although above calculations give a fair understanding of magnetic properties of the martensitic state in $Mn_2NiIn$ type alloys, they do not give explain the complete suppression of martensitic transformation with small changes in the Mn:Ni ratio. In $Mn_2Ni_{1+x}In_{1-x}$, though alloy with $x = 0.6$ undergoes martensitic transformation at 232 K, the alloy $Mn_{2.08}Ni_{1.52}In_{0.4}$ does not exhibit any martensitic transformation down to 4 K. At the same time, $Mn_{1.92}Ni_{1.68}In_{0.4}$ exhibits martensitic transformation at a higher temperature of 250 K. To understand the possible cause of such a drastic variation of martensitic transformation temperatures in these alloys, a linear component fitting (LCF) analysis was performed on the experimental data recorded at the Mn and Ni K edge XAFS in the above three compositions using the FEFF calculated XAFS of Ni and Mn occupying different site positions as per MODEL A and MODEL B with a distortion of 0.1 Å. As per MODEL A, Ni would be found at X and Z sites, while Mn would be present at X and Y sites. In the case of MODEL B, Ni would be present only at X sites and Mn would occupy all the three sites. The calculated XAFS of Ni and Mn for each site was used as standards, and Athena was employed to give a best possible combination that describes the experimental data in $Mn_{2-y}Ni_{1.6+y}In_{0.4}$. Based on this LCF analysis, the obtained site occupancies of Ni and Mn are presented in Tables II and III, respectively.

It is interesting to note that in the case of $Mn_{2.08}Ni_{1.92}In_{0.4}$ alloy that does not undergo martensitic transformation, Mn is found to be only at X and Y sites, while Ni is present at the Z site. In the case of the other two alloys, Ni primarily occupies X sites, while Mn is found to occupy all the three sites. The presence of Mn at the Z site along with a local structural distortion in its position gives rise to a shorter Ni-Mn bond as compared to Ni-In and Ni(3d)–Mn(3d) hybridization, which plays an important role in martensitic transformation in $Ni_2Mn_{1+x}In_{1-x}$ alloys. A clear differentiation between site occupancies of $Mn_2NiIn$ type alloys undergoing martensitic transformation and non-martensitic alloys highlights the importance of antisite disorder along with local structural distortion in inducing martensitic transformation in these alloys.

TABLE II. LCF analysis for Ni K edge XAFS. The bracketed letters indicate the crystallographic site positions.

| | Ni EXAFS | | |
|---|---|---|---|
| Sample | Model (position) | Ni-Mn(Z) bond distancedisorder | Species concentration |
| $Mn_{2.08}Mn_{1.52}In_{0.4}$ | A(X) | … | 79 ± 20 |
| | A(Z) | … | 14 ± 07 |
| | B(X) | 0.1 | 12 ± 14 |
| $Mn_2Ni_{1.6}In_{0.4}$ | A(X) | … | 83 ± 13 |
| | B(X) | 0.1 | 17 ± 11 |
| $Mn_{1.92}Ni_{1.68}In_{0.4}$ | A(X) | … | 86 ± 14 |
| | B(X) | 0.1 | 14 ± 13 |

TABLE III. LCF analysis for Mn K edge XAFS. The bracketed letters indicate the crystallographic site positions.

| | Mn EXAFS | | |
|---|---|---|---|
| Sample | Model (position) | Ni-Mn(Z) bond distance disorder | Species concentration |
| $Mn_{2.08}Ni_{1.52}$ $In_{0.4}$ | A(X) | … | 62 ± 05 |
| | B(Y) | 0.1 | 38 ± 05 |
| $Mn_2Mn_{1.6}In_{0.4}$ | A(X) | … | 49 ± 6 |
| | B(Y) | 0.1 | 31 ± 10 |
| | B(Z) | 0.1 | 20 ± 07 |
| $Mn_{1.92}Ni_{1.68}In_{0.4}$ | A(X) | … | 50 ± 25 |
| | B(Y) | 0.1 | 23 ± 5.4 |
| | B(Y) | 0.1 | 27 ± 7.7 |

## IV. CONCLUSION

We have carried out *ab-initio* calculations at the Ni and Mn K edges to understand the driving force for martensitic transformation in $Mn_2Ni_{1+x}In_{1-x}$ alloys. The presence of Mn at Z sites appears to be the main requirement for the alloy composition to undergo martensitic transformation. The *ab-initio* XAFS calculations indicate preferential occupation of X sites by Ni atoms, while Mn atoms occupy all X, Y, and Z sites of the $X_2YZ$ Heusler structure. Such a site occupancy disorder of Mn atoms is in addition to a local structural disorder due to size differences between Mn and In atoms, which is also present in $Ni_2Mn_{1+x}In_{1-x}$ alloys. This agrees well with the observed similarities in magnetic properties of the martensitic state of $Mn_2Ni_{1+x}In_{1-x}$ and $Ni_2Mn_{1+x}In_{1-x}$ alloys. Further, the drastic suppression of martensitic transformation with small changes in the composition in $Mn_{2-y}Ni_{1.6+y}In_{0.4}$ can also be understood based on the occupancy of Mn at Z sites. $Mn_{2.08}Ni_{1.52}In_{0.4}$, which has no Mn atoms at the Z site, does not undergo martensitic transformation, while $Mn_2Ni_{1.6}In_{0.4}$, which has about 20% Z site occupancy of Mn, undergoes martensitic transformation at about 230 K.

## ACKNOWLEDGMENTS

The authors would like to acknowledge the financial assistance from Science and Engineering Research Board (SERB), DST, Government of India, under the Project No. SB/S2/CMP-096/2013. The work at Photon Factory was performed under the Proposal No. 2011G0077.

[1]T. Krenke, E. Duman, M. Acet, E. F. Wasserman, X. Moya, L. Mañosa, and A. Planes, Nat. Mater. **4**, 450 (2005).
[2]P. A. Bhobe, K. R. Priolkar, and A. K. Nigam, Appl. Phys. Lett. **91**, 242503 (2007).
[3]M. Khan, I. Dubenko, S. Stadler, and N. Ali, J. Appl. Phys. **102**, 113914 (2007).
[4]J. Du, Q. Zheng, W. J. Ren, W. J. Feng, X. G. Liu, and Z. D. Zhang, J. Phys. D **40**, 5523 (2007).
[5]J. Liu, N. Scheerbaum, J. Lyubina, and O. Gutfleisch, Appl. Phys. Lett. **93**, 102512 (2008).
[6]M. Khan, N. Ali, and S. Stadler, J. Appl. Phys. **101**, 053919 (2007).
[7]I. Dubenko, M. Khan, A. K. Pathak, B. R. Gautam, S. Stadler, and N. Ali, J. Magn. Magn. Mater. **321**, 754 (2009).
[8]A. K. Nayak, K. G. Suresh, and A. K. Nigam, J. Appl. Phys. **107**, 09A927 (2010).
[9]Z. D. Han, D. H. Wang, C. L. Zhang, H. C. Xuan, B. X. Gu, and Y. W. Du, Appl. Phys. Lett. **90**, 042507 (2007).
[10]V. K. Sharma, M. K. Chattopadhyay, R. Kumar, T. Ganguli, P. Tiwari, and S. B. Roy, J. Phys. Condens. Matter **19**, 496207 (2007).
[11]P. J. Shamberger and F. S. Ohuchi, Phys. Rev. B **79**, 144407 (2009).
[12]V. D. Buchelnikov and V. V. Sokolovskiy, Phys. Met. Metallogr. **112**, 633 (2011).
[13]Z. Li, C. Jing, J. Chen, S. Yuan, S. Cao, and J. Zhang, Appl. Phys. Lett. **91**, 112505 (2007).
[14]H. C. Xuan, Q. Q. Cao, C. L. Zhang, S. C. Ma, S. Y. Chen, D. H. Wang, and Y. W. Du, Appl. Phys. Lett. **96**, 202502 (2010).
[15]N. M. Bruno, C. Yegin, I. Karaman, J.-H. Chen, J. H. Ross, Jr., J. Liu, and J. Li, Acta Mater. **74**, 66 (2014).
[16]J.-H. Chen, N. M. Bruno, I. Karaman, Y. Huang, J. Li, and J. H. Ross, Jr., Acta Mater. **105**, 176 (2016).
[17]J.-H. Chen, N. M. Bruno, I. Karaman, Y. Huang, J. Li, and J. H. Ross, Jr., J. Appl. Phys. **116**, 203901 (2014).
[18]K. Koyama, K. Watanabe, T. Kanomata, R. Kainuma, K. Oikawa, and K. Ishida, Appl. Phys. Lett. **88**, 132505 (2006).
[19]R. Kainuma, Y. Imano, W. Ito, Y. Sutou, H. Morito, S. Okamoto, O. Kitakami, K. Oikawa, A. Fujita, T. Kanomata, and K. Ishida, Nature(London) **439**, 957 (2006).
[20]R. Kainuma, Y. Imano, W. Ito, H. Morito, Y. Sutou, K. Oikawa, A. Fujita, K. Ishida, S. Okamoto, O. Kitakami, and T. Kanomata, Appl. Phys. Lett. **88**, 192513 (2006).
[21]K. Haldar, D. C. Lagoudas, and I. Karaman, J. Mech. Phys. Solids **69**, 33 (2014).
[22]H. E. Karaca, I. Karaman, B. Basaran, Y. Ren, Y. I. Chumlyakov, and H. J. Maier, Adv. Funct. Mater. **19**, 983 (2009).
[23]H. Karaca, I. Karaman, B. Basaran, Y. Chumlyakov, and H. Maier, Acta Mater. **54**, 233 (2006).
[24]T. Krenke, E. Duman, M. Acet, E. F. Wassermann, X. Moya, L. Mañosa, A. Planes, E. Suard, and B. Ouladdiaf, Phys. Rev. B **75**, 104414 (2007).
[25]V. V. Khovaylo, V. D. Buchelnikov, R. Kainuma, V. V. Koledov, M. Ohtsuka, V. G. Sharov, T. Takagi, S. V. Taskaev, and A. N. Vasiliev, Phys. Rev. B **72**, 224408 (2005).
[26]V. D. Buchelnikov, V. V. Sokolovskiy, H. C. Herper, H. Ebert, M. E. Gruner, S. V. Taskaev, V. V. Khovaylo, A. Hucht, A. Dannenberg, M. Ogura, H. Akai, M. Acet, and P. Entel, Phys. Rev. B **81**, 094411 (2010).
[27]T. Kanomata, Y. Kitsunai, K. Sano, Y. Furutani, H. Nishihara, R. Y. Umetsu, R. Kainuma, V. Miura, and M. Shirai, Phys. Rev. B **80**, 214402 (2009).
[28]V. V. Khovaylo, T. Kanomata, T. Tanaka, M. Nakashima, Y. Amako, R. Kainuma, R. Y. Umetsu, H. Morito, and H. Miki, Phys. Rev. B **80**, 144409 (2009).
[29]M. Ye, A. Kimura, Y. Miura, M. Shirai, Y. T. Cui, K. Shimada, H. Namatame, M. Taniguchi, S. Ueda, K. Kobayashi, R. Kainuma, T. Shishido, K. Fukushima, and T. Kanomata, Phys. Rev. Lett. **104**, 176401 (2010).
[30]M. Kataoka, K. Endo, N. Kudo, T. Kanomata, H. Nishihara, T. Shishido, R. Y. Umetsu, M. Nagasako, and R. Kainuma, Phys. Rev. B **82**, 214423 (2010).
[31]J. Monroe, J. Raymond, X. Xu, M. Nagasako, R. Kainuma, Y. Chumlyakov, R. Arroyave, and I. Karaman, Acta Mater. **101**, 107 (2015).
[32]P. J. Webster, K. R. A. Ziebeck, S. L. Town, and M. S. Peak, Philos. Mag. Part B **49**, 295 (1984).
[33]C. Hurd and S. McAlister, J. Magn. Magn. Mater. **61**, 114 (1986).
[34]P. J. Brown, A. P. Gandy, K. Ishida, W. Ito, R. Kainuma, T. Kanomata, K. U. Neumann, K. Oikawa, B. Ouladdiaf, A. Sheikh, and K. R. A. Ziebeck, J. Phys.: Condens. Matter **22**, 096002 (2010).
[35]S. Chadov, J. Kiss, and C. Felser, Adv. Funct. Mater. **23**, 832 (2013).
[36]K. R. Priolkar, D. N. Lobo, P. A. Bhobe, S. Emura, and A. K. Nigam, Eur. Phys. Lett. **94**, 38006 (2011).
[37]K. R. Priolkar, P. A. Bhobe, D. N. Lobo, S. W. D'Souza, S. R. Barman, A. Chakarabarti, and S. Emura, Phys. Rev. B **87**, 144412 (2013).
[38]G. D. Liu, X. F. Dai, S. Y. Yu, Z. Y. Zhu, J. L. Chen, G. H. Wu, H. Zhu, and J. Q. Xiao, Phys. Rev. B **74**, 054435 (2006).
[39]G. D. Liu, J. L. Chen, Z. H. Liu, X. F. Dai, G. H. Wu, B. Zhang, and X. X. Zhang, Appl. Phys. Lett. **87**, 262504 (2005).
[40]S. R. Barman, S. Banik, A. K. Shukla, C. Kamal, and A. Chakrabarti, EPL (Europhys. Lett.) **80**, 57002 (2007).
[41]S. R. Barman and A. Chakrabarti, Phys. Rev. B **77**, 176401 (2008).
[42]S. Paul and S. Ghosh, J. Phys.: Condens. Matter **23**, 206003 (2011).
[43]L. Ma, S. Q. Wang, Y. Z. Li, C. M. Zhen, D. L. Hou, W. H. Wang, J. L. Chen, and G. H. Wu, J. Appl. Phys. **112**, 083902 (2012).

[44]J. L. Sánchez Llamazares, B. Hernando, V. M. Prida, C. García, J. González, R. Varga, and C. A. Ross, J. Appl. Phys. **105**, 07A945 (2009).
[45]D. N. Lobo, S. Dwivedi, C. A. daSilva, N. O. Moreno, K. R. Priolkar, and A. K. Nigam, J. Appl. Phys. **114**, 173910 (2013).
[46]A. Ayuela, J. Enkovaara, K. Ullakko, and R. M. Nieminen, J. Phys.: Condens. Matter **11**, 2017 (1999).
[47]S. Singh, R. Rawat, S. E. Muthu, S. W. D'Souza, E. Suard, A. Senyshyn, S. Banik, P. Rajput, S. Bhardwaj, A. M. Awasthi, R. Ranjan, S. Arumugam, D. L. Schlagel, T. A. Lograsso, A. Chakrabarti, and S. R. Barman, Phys. Rev. Lett. **109**, 246601 (2012).
[48]A. K. Nayak, M. Nicklas, S. Chadov, C. Shekhar, Y. Skourski, J. Winterlik, and C. Felser, Phys. Rev. Lett. **110**, 127204 (2013).
[49]C. L. Tan, Y. W. Huang, X. H. Tian, J. X. Jiang, and W. Cai, Appl. Phys. Lett. **100**, 132402 (2012).
[50]S. I. Zabinsky, J. J. Rehr, A. Ankudinov, R. C. Albers, and M. J. Eller, Phys. Rev. B **52**, 2995 (1995).
[51]C.-M. Li, H.-B. Luo, Q.-M. Hu, R. Yang, B. Johansson, and L. Vitos, Phys. Rev. B **84**, 174117 (2011).
[52]T. J. Burch, T. Litrenta, and J. I. Budnick, Phys. Rev. Lett. **33**, 421 (1974).
[53]S. Podgornykh, S. Streltsov, V. Kazantsev, and E. Shreder, J. Magn. Magn. Mater. **311**, 530 (2007).
[54]D. N. Lobo, K. R. Priolkar, P. A. Bhobe, D. Krishnamurthy, and S. Emura, Appl. Phys. Lett. **96**, 232508 (2010).